200500610A

厚生労働科学研究研究費補助金

感覚器障害研究事業

網膜血管新生抑制機構の解明とその応用に関する研究

平成１７年度　総括・分担研究報告書

主任研究者　細谷　健一

平成１８（２００６）年　３月

目　次

厚生労働科学研究費補助金（感覚器障害研究事業）
総括研究報告書

網膜ペリサイト由来シンタキシン 2D の同定と血管内皮細胞増殖抑制効果

主任研究者　細谷　健一　富山大学・薬学部　教授

研究要旨：本研究は、網膜ペリサイト由来の網膜血管内皮細胞の増殖抑制因子を同定し、そのメカニズム解明を目的とした。網膜ペリサイト株(TR-rPCT)培養濃縮液をゲルろ過法によって分画し、TR-iBRB 細胞の増殖抑制活性を示した画分を二次元電気泳動法で分離した。さらに、MALDI-TOFMS/peptide mass fingerprinting 法解析からシンタキシン 2D が同定された。タンパク質をコードする遺伝子を TR-rPCT 細胞から単離後、大腸菌 BL21 に導入してリコンビナントタンパク質を作製した。シンタキシン 2D の網膜毛細血管内皮細胞増殖抑制効果の 50%阻害濃度は約 6 μM であった。シンタキシン 2D は網膜血管内皮細胞にアポトーシスを誘導することが示唆された。

分担研究者　笹岡　利安　富山大学・薬学研究科　教授

A．研究目的

糖尿病網膜症は、２大中途失明原因のひとつであり、高齢化社会を迎える日本において、失明への予防法と新たな治療薬開発が望まれている。糖尿病網膜症における血管新生は、網膜血管の周囲にあるペリサイトの脱落から始まっており、網膜ペリサイトから分泌される因子が網膜血管内皮細胞の増殖を制御していると仮説を立てた。我々が樹立した条件的不死化網膜血管内皮細胞株(TR-iBRB)と網膜ペリサイト株(TR-rPCT)の共培養解析の結果、TR-rPCT 細胞培養濃縮液を TR-iBRB 細胞に添加すると増殖が著しく抑制されることを見いだした。

そこで本研究では、網膜ペリサイトから分泌される網膜血管内皮細胞増殖抑制因子を同定し、網膜血管新生抑制機構を解明することを目的とした。

B．研究方法

TR-rPCT 細胞を Dulbecco's modified Eagle's medium (DMEM)で培養し、培養濃縮液は培養液上清を限外濾過法によって調製した。培養濃縮液からのタンパク質精製は、硫安沈殿させたタンパク質を陰イオン交換クロマトグラフィー、ハイドロキシアパタイトクロマトグラフィーでフラクションに分離した。各フラクションの細胞増殖抑制効果は TR-iBRB 細胞における 5-bromo-2'-deoxyuridine(BrdU)の取り込みによる DNA 合成活性から判定した。細胞増殖抑制効果の高いフラクションを二次元電気泳動で分離後、マトリックス支援レーザー脱離イオン化飛行時間型質量分析装

置（MALDI-TOFMS）で質量ならびにアミノ酸配列を解析した。さらに、Peptide Mass Fingerprinting (PMF)解析、データベース（GenBank）を活用し、全アミノ酸配列を決定した。同定されたタンパク質をコードする遺伝子をTR-rPCT細胞から単離後、大腸菌BL21に導入してリコンビナントタンパク質を作製し、TR-iBRB細胞増殖抑制活性の解析を行った。

C．研究結果

TR-rPCT細胞の培養濃縮液タンパク質は60のフラクションに分離した。60のフラクションの中でNo. 31-35のフラクション付近でBrdUの強い取り込み抑制が示された。このフラクションタンパク質を二次元電気泳動にて分離し、MALDI-TOFMS、PMF解析からシンタキシン2Dであることが示唆された。ラットシンタキシン2Dを特異的に認識するプライマーを用いてRT-PCR法でオープンリーディングフレーム（ORF）のクローニングを行った。その結果、ラット網膜およびTR-rPCT細胞にシンタキシン2DをコードするmRNAが発現していることが示された。さらに、シンタキシン2アイソフォームを認識する抗体を用いた解析から、シンタキシン2DはTR-rPCT細胞に発現し、培養液中にも存在していることが示唆された。

シンタキシン2Dのリコンビナントタンパク質を作製するために、目的遺伝子のORFを発現誘導ベクターに導入し、大腸菌にて大量に培養した。タンパク質は大腸菌から収集、精製した。精製したタンパク質はMALDI-TOFMSによってタンパク質の質量を、プロテインシークエンサーを用いてN末端アミノ酸配列解析を行い、単離したタンパク質と同一であることを確認した。

シンタキシン2Dは濃度依存的にTR-iBRB細胞の増殖を抑制し、50%阻害濃度は5.95 μMであった。さらに、シンタキシン2DはTR-iBRB細胞にアポトーシスを誘導することが示唆された。

D．考察

TR-rPCT細胞培養濃縮液からTR-iBRB細胞増殖抑制効果を示すタンパク質としてシンタキシン2Dを単離した。このタンパク質はTR-rPCT細胞、ラット網膜に発現していることが示された。シンタキシン2DはTR-iBRB細胞にアポトーシスを誘導し、増殖抑制効果を示すことから、他の内皮細胞増殖抑制因子とは異なったメカニズムであることが示唆された。今後、効果発現の様式、in vivoにおける薬理効果を研究することで糖尿病網膜症治療薬として開発につながるものと思われる。

E．結論

本研究によって、網膜ペリサイトから分泌される網膜血管内皮細胞増殖因子の1つとしてシンタキシン2Dの関与を明らかにした。物質の同定のみならず、リコンビナントタンパク質を作製にも成功した。今後は、薬理効果を証明する予定である。

F．健康危険情報

特になし

G．研究発表

1．論文発表

Ohtsuki S, Tomi M, Hata T, Nagai Y, Hori S, Mori S, Hosoya K, Terasaki T, Dominant expression of androgen receptor and its functional regulation of organic anion transporter 3 in rat brain capillary endothelial cells; comparison of gene expression between the blood-brain and -retinal barriers. *J. Cell. Physiol.*, 204, 896-900 (2005).

Fukui K, Wada T, Kagawa S, Nagira K, Ikubo M, Ishihara H, Kobayashi M, Sasaoka T, Impact of the liver-specific expression of SHIP2 (SH2-containing inositol 5'-phosphatase 2) on insulin signaling and glucose metabolism in mice. *Diabetes*, 54, 1958-1967 (2005)

Nakashima T, Tomi M, Tachikawa M, Watanabe M, Terasaki T, Hosoya K, Evidence for creatine biosynthesis in Müller glia. *Glia*, 52, 47-52 (2005).

Zhou J, Deo BK, Hosoya K, Terasaki T, Obrosova IG, Brosius III FC, Kumagai AK, Increased JNK phosphorylation and oxidative stress in response to increased glucose flux through increased GLUT1 expression in rat retinal endothelial cells. *Invest. Ophthalmol. Vis. Sci.*, 46, 3403-3410 (2005).

2．学会発表

Leal EC, Manivannan A, Aveleira C, Serra A, Castilho A, Terasaki T, Hosoya K, Cotter M, Ambrosio AF, Forrester JV, Leukocyte adhesion and blood retinal barrier (BRB) breakdown in diabetic retinopathy (DR): Role of nitric oxide (NO), The Association of Research in Vision and Ophthalmolgy, May 2005, Fort Lauderdale USA.

Ola MS, Barber A, Hosoya K, LaNoue K, Hydrocortisone regulates the expression of glutamine synthetase (GS) and aspartate/glutamate carrier (AGC) in cultured rat retinal Müller cells (TR-MUL), The Association of Research in Vision and Ophthalmolgy, May 2005, Fort Lauderdale USA.

Ambrosio AF, Leal EC, Manivannan A, Aveleira C, Serra A, Castilho A, Terasaki T, Hosoya K, Cotter M, Forrester JV, The involvement of nitric oxide in leukocyte adhesion and blood retinal barrier breakdown in diabetic retinopathy, 15th meeting of European Association for the Study of Diabetes-eye Complications Study Group (EASDEC), May 2005, Coimba, Portugal.

Hosoya K, Kiyokawa J, Tachikawa M, Kondo T, Ohtsuki S, Terasaki T, Tomi M, Retinal endotheial cell growth suppression by retinal pericyte-secreted proteins, US-Japan Conference on Drug

Development Rational Drug Design, July 2005, Los Angeles USA.

Hosoya K, Blood-retinal barrier transport biology, Moving Targets 2005: 4th Annual Multidisciplinary Scientific Symposium, August 2005, Los Angeles USA.

Hosoya K, Tajima A, Tachikawa M, Tomi M: GABA transport at the inner blood-retinal barrier, 13th NA ISSX/20th JSSX Meeting, October 2005, Maui, USA.

Hosoya K, Kiyokawa J, Tachikawa M, Kondo T, Ohtsuki S, Terasaki T, Tomi M, The role of retinal pericyte-secreted proteins in suppressing retinal endothelial cell growth, AAPS annual meeting and exposition, November 2005, Nashville USA.

清川順平，松本悠，登美斉俊，立川正憲，近藤撤，大槻純男，寺崎哲也，細谷健一，網膜周皮細胞分泌タンパク質による網膜内皮細胞増殖抑制，日本薬学会北陸支部第 113 回例会，2005 年 11 月，金沢.

H．知的財産権の出願・登録情報

１．特許取得　なし

２．実用新案登録　なし

３．その他　なし

厚生労働科学研究費補助金（感覚器障害研究事業）
分担研究報告書

網膜血管内皮細胞に発現するLAT1を介した必須アミノ酸輸送とその制御メカニズム

分担研究者　登美　斉俊　富山大学・薬学部　助手
分担研究者　立川　正憲　富山大学・薬学部　助手

研究要旨：中性アミノ酸トランスポーターであるLAT1は新生血管内皮細胞に特に強く発現し、癌組織への必須アミノ酸供給に重要な役割を果たしている。本研究は網膜血管内皮細胞におけるLAT1の機能発現、およびその虚血時における制御機構の解明を目的とした。LAT1の代表的基質である[^{3}H]L-leucineのラット網膜取り込みクリアランスは203 μL/(min· g retina) であり、L-leucineは循環血液から網膜へ輸送されることが示された。網膜血管内皮細胞のモデル細胞株、TR-iBRB細胞におけるL-leucine輸送特性はLAT1の特性と一致した。In vivo網膜血管内皮細胞においてLAT1の発現が示され、さらにmRNAレベルではLAT2に比べてLAT1の発現量が著しく高いことが示された。グルコース枯渇条件下のTR-iBRB細胞においてLAT1 mRNA発現量の増加および[^{3}H]L-leucine取り込み速度の上昇、さらにLAT1遺伝子promoter活性の上昇が示された。したがって、網膜血管内皮細胞にはLAT1を介したleucineなど必須アミノ酸供給機構が機能し、さらに本機構はグルコース枯渇時には活性化することが示された。以上から、網膜血管新生阻害剤の有力な標的分子としてLAT1を提示することができた。

A．研究目的

糖尿病網膜症に伴って生じる網膜新生血管には大量の糖およびアミノ酸を必要とするが、それら栄養素の細胞内取り込みは細胞膜において機能するトランスポーターが担当している。特に、細胞内代謝で産生出来ない必須アミノ酸を獲得するためのアミノ酸トランスポーターの存在は必須であり、網膜血管新生の律速段階の一つを形成している可能性が高い。中性アミノ酸トランスポーター、LAT1はleucineをはじめとする数多くの必須アミノ酸を基質とし、癌組織において新生血管に特に強く発現し、癌組織に対する必須アミノ酸供給に重要な役割を果たしていることが知られている。従って、網膜血管内皮細胞においてLAT1が発現している場合、必須アミノ酸の細胞内への供給に不可欠な役割を果たしていると考えられ、網膜血管新生阻害剤の有力な標的分子となりうる。さらに、糖尿病網膜症に伴う網膜血管新生には血管障害による虚血が深く関与しており、栄養素が枯渇した虚血状態におけるLAT1の発現制御を明らかにすることは、LAT1を通じた網膜血管新生抑制の戦略を考える上で極めて重要である。

そこで、本研究では網膜血管内皮細胞における LAT1 の機能発現を明らかにすること、さらにその虚血による機能制御メカニズムを解明することを目的とした。

B．研究方法

ラット大腿静脈から[^{3}H]L-leucine を投与した後、一定時間後に採血および臓器摘出を行い、[^{3}H]L-leucine の組織血漿間分配係数($K_{p,app}$)を算出した。さらに、integration plot 法を用いて見かけの[^{3}H]L-leucine 網膜取り込みクリアランスを算出した。TR-iBRB 細胞は網膜毛細血管内皮細胞の in vitro モデル細胞として用いた。TR-iBRB 細胞における L-leucine 輸送機構は、37°C における [^{3}H]L-leucine 取り込みから解析した。網膜血管内皮細胞は、ラット網膜ホモジネートを酵素処理後、磁気標識抗 CD31 抗体と混合して内皮細胞を磁気標識し、磁石を用いて単離した。LAT1 の発現は免疫染色法、Western blot 法、RT-PCR 法、およびリアルタイム定量 PCR 法を用いて解析した。ラットゲノム DNA ライブラリーから PCR 法を用いて LAT1 遺伝子プロモーター配列(-1958/+70)を増幅し、ルシフェラーゼ遺伝子を有する pGL3-Basic プラスミドに挿入した(LAT1 promoter/pGL3 プラスミド)。構築したプラスミドを TR-iBRB 細胞に導入し、ルミノメーターを用いたルシフェラーゼアッセイにより LAT1 プロモーター活性を測定した。

C．研究結果

ラット網膜への L-leucine 移行性を解析するため、integration plot 法を用いた in vivo 解析を行った。見かけの[^{3}H]L-leucine 網膜取り込みクリアランスは 203 μL/(min·g retina) であることが示された。

TR-iBRB2 細胞における[^{3}H]L-leucine 取り込みは 10 分までは直線性を示し、その取り込みは Na^+および Cl^-非依存性を示した。TR-iBRB2 細胞における L-leucine 取り込みは濃度依存性を示し、得られた Michaelis-Menten 定数 (K_m) は 14.1 μM であった。さらに、[^{3}H]L-leucine の取り込みは LAT1、LAT2 に共通の基質である L-leucine、L-phenylalanine、L-methionine、L-valine 、 L-isoleucine 、 L-tyrosine 、 L-tryptophan および 2-aminobicyclo-(2,2,1)-heptane-2-carboxylic acid (BCH)に加え、LAT1 のみの基質である D-leucine、D-phenylalanine および D-methionine によって 50%以上阻害された。一方、LAT2 のみの基質である L-alanine および L-glutamine によっては 30%程度の阻害にとどまった。

磁気標識抗 CD31 抗体を用いて単離した網膜血管内皮細胞および TR-iBRB 細胞において LAT1 および LAT2 mRNA の発現が共に示されたが、LAT1 mRNA の発現量は LAT2 と比較して各々15 倍および 100 倍高いことが示された。TR-iBRB 細胞および初代培養ヒト網膜血管内皮細胞には LAT1 タンパク質が発現していることが示された。さらに、凍結網膜切片に対する免疫染色解析から、in vivo ラット網膜毛細血管内皮細胞に LAT1 が発現していることが示された。

酸素濃度 1%の低酸素条件およびグルコース非含有培地を用いた glucose 枯渇条件のそれぞれで培養した TR-iBRB 細胞を虚血状態の in vitro モデルとした。低酸素条

件下で24時間培養したTR-iBRB細胞において、LAT1 mRNAの発現量は変動せず、[3H]L-leucineの取り込みについても1.6倍の増加であった。一方、グルコース枯渇条件下におけるLAT1 mRNAの発現、および[3H]L-leucineの取り込みは処理時間依存的に増加し、処理時間24時間においてLAT1 mRNAは4.0倍、および[3H]L-leucineの取り込みは2.6倍に増加した。グルコース枯渇条件下におけるmRNA発現誘導および取り込み活性化は転写阻害剤actinomycin Dによって抑制され、取り込み活性化については翻訳阻害剤cycloheximideによっても抑制された。

LAT1 promoter/pGL3プラスミドを導入したTR-iBRB細胞においてルシフェラーゼアッセイを用いた転写活性解析を行った結果、controlプラスミド導入細胞に比べて数十倍高い転写活性が示された。さらに、グルコース枯渇条件下では通常培養条件と比較して2倍高いことが示された。

D．考察

ラットにおける見かけの[3H]L-leucine網膜取り込みクリアランスは203 μL/(min·g retina)であり、L-leucineは循環血液から網膜へ輸送されていることが示された。TR-iBRB細胞におけるL-leucine取り込みはNa^+およびCl^-非依存性およびK_m値14.1 μMの濃度依存性を示した。この値は、ラットLAT1および4F2hcをアフリカツメガエル卵母細胞に発現させて解析したK_m値（18 μM）と近似したが、LAT2と4F2hcに対して同様に発現解析を行ったK_m値（120 μM）とは異なった。TR-iBRB細胞におけるL-leucine輸送に対するLAT1選択的基質による阻害は、LAT2選択的基質による阻害に比べて強いことが示された。さらに、in vivo網膜血管内皮細胞においてLAT1の発現が示され、mRNAレベルではLAT2の発現量に比べてLAT1の発現量が著しく高いことが示された。したがって、網膜血管内皮細胞においてLAT1が発現し、必須アミノ酸の輸送において主要な役割を果たしていることが示唆された。

グルコース枯渇条件下のTR-iBRB細胞においてLAT1 mRNAの発現量増加および[3H]L-leucine取り込みの活性化が示され、これらは転写阻害剤によって阻害された。さらに、LAT1プロモーター活性はグルコース枯渇条件で上昇することが示された。したがって、TR-iBRB細胞においてグルコース枯渇による転写レベルにおける遺伝子発現制御が起こり、LAT1の発現が誘導されることが示唆された。

E．結論

本研究によって、網膜血管内皮細胞にはLAT1が発現し、leucineなど必須アミノ酸の輸送を担っていることが示唆された。さらに、グルコース枯渇時にはLAT1遺伝子の転写が活性化し、その発現が誘導されることが示された。したがって、LAT1は虚血とそれに伴う血管新生時における旺盛なアミノ酸需要に応える役割を果たしている可能性が高い。以上から、LAT1を標的分子とした阻害剤を開発し、網膜血管内皮細胞への必須アミノ酸供給を遮断することで血管新生を抑制するという、網膜血管新生治療に向けた新戦略を提示することができた。

F．健康危険情報

特になし

G．研究発表

1．論文発表

Tomi M, Mori M, Tachikawa M, Katayama K, Terasaki T, Hosoya K. L-Type amino acid transporter 1 (LAT1)-mediated L-leucine transport at the inner blood-retinal barrier. *Invest. Ophthalmol. Vis. Sci.*, 46, 2522-2530 (2005).

2．学会発表

Hosoya K, Mori M, Katayama K, Tachikawa M, Tomi M. The role of LAT1 at the inner blood-retinal barrier in supplying large neutral amino acids. Annual meeting of the Association for Research in Vision and Ophthalmology, May 2005, Fort Lauderdale USA.

Hosoya K, Mori M, Katayama K, Tachikawa M, Terasaki T, Tomi M. Expression and transport function of LAT1 at the inner blood-retinal barrier. Retronetabolism Based Drug Design and Targeting 5th Cenferance, May 2005, Hakone.

Nakamura G, Tomi M, Katayama K, Hosoya K. Influx and efflux transport of vitamin C in retinal Müller cells. US-Japan Conference on Drug Development Rational Drug Design, August 2005, Los Angeles USA.

Tomi M, Mori M, Tachikawa M, Katayama K, Hosoya K. LAT1 as a system responsible for the transport of L-leucine at the inner blood-retinal barrier. US-Japan Conference on Drug Development Rational Drug Design, August 2005, Los Angeles USA.

Tomi M, Terayama T, Isobe T, Ohtsuki S, Terasaki T, Hosoya K. Expression and function of taurine transporter at the inner blood-retinal barrier. 13th NA ISSX/20th JSSX Meeting, October 2005, Maui USA.

Tomi M, Tajima A, Tachikawa M, Hosoya K. The role of taurine transporter in GABA transport at the inner blood-retinal barrier. 第 27 回生体膜と薬物の相互作用シンポジウム, 2005 年 11 月, 京都.

H．知的財産権の出願・登録情報

1．特許取得　なし

2．実用新案登録　なし

3．その他　なし

研究成果の刊行に関する一覧表

発表者氏名	論文タイトル名	発表誌名	巻号	ページ	出版年
Ohtsuki S, Tomi M, Hata T, Nagai Y, Hori S, Mori S, Hosoya K, Terasaki T.	Dominant expression of androgen receptor and its functional regulation of organic anion transporter 3 in rat brain capillary endothelial cells; comparison of gene expression between the blood-brain and -retinal barriers.	J. Cell. Physiol.	204	896-900	2005
Fukui K, Wada T, Kagawa S, Nagira K, Ikubo M, Ishihara H, Kobayashi M, Sasaoka T.	Impact of the liver-specific expression of SHIP2 (SH2-containing inositol 5'-phosphatase 2) on insulin signaling and glucose metabolism in mice.	Diabetes	54	1958-1967	2005
Nakashima T, Tomi M, Tachikawa M, Watanabe M, Terasaki T, Hosoya K.	Evidence for creatine biosynthesis in Müller glia.	Glia	52	47-52	2005
Zhou J, Deo BK, Hosoya K, Terasaki T, Obrosova IG, Brosius III FC, Kumagai AK.	Increased JNK phosphorylation and oxidative stress in response to increased glucose flux through increased GLUT1 expression in rat retinal endothelial cells.	*Invest. Ophthalmol. Vis. Sci.*	46	3403-3410	2005
Tomi M, Mori M, Tachikawa M, Katayama K, Terasaki T, Hosoya K.	L-type amino acid transporter 1-mediated L-leucine transport at the inner blood-retinal barrier	*Invest. Ophthalmol. Vis. Sci.*	10	2522-2530	2005

JOURNAL OF CELLULAR PHYSIOLOGY 204:896–900 (2005)

Dominant Expression of Androgen Receptors and Their Functional Regulation of Organic Anion Transporter 3 in Rat Brain Capillary Endothelial Cells; Comparison of Gene Expression Between the Blood–Brain and -Retinal Barriers

SUMIO OHTSUKI,[1,2,3] MASATOSHI TOMI,[3,4] TOSHIO HATA,[1] YOKO NAGAI,[1] SATOKO HORI,[1,2,3] SHINOBU MORI,[1] KEN-ICHI HOSOYA,[3,4] AND TETSUYA TERASAKI[1,2,3]*

[1]*Department of Molecular Biopharmacy and Genetics, Graduate School of Pharmaceutical Sciences, Sendai, Japan*
[2]*New Industry Creation Hatchery Center, Tohoku University, Sendai, Japan*
[3]*CREST and SORST of the Japan Science and Technology Agency (JST), Japan*
[4]*Faculty of Pharmaceutical Sciences, Toyama Medical and Pharmaceutical University, Toyama, Japan*

Brain and retinal capillary endothelial cells (BCECs and RCECs, respectively) exhibit a barrier structure and function. Comparison of gene expression in these cells could clarify the selective function of each barrier. The purpose of this study was to identify the genes selectively expressed at the blood–brain barrier (BBB) and to clarify the function of the selective gene, androgen receptor (AR). Gene expression was compared by a differential display using conditionally immortalized rat BCECs and RCECs (TR-BBB and TR-iBRB, respectively). A total of 12 gene fragments were identified as the selective genes dominantly expressed in TR-BBB cells. The most selective fragment in TR-BBB cells had the highest homology with the 3′-UTR of human and mouse AR. Rat AR mRNA was detected in TR-BBB cells and the brain capillary rich fraction, but not in TR-iBRB cells. Expression of organic anion transporter 3 (OAT3) mRNA in TR-BBB cells was induced by treatment with dihydrotestosterone (DHT), an AR ligand, and this induction was suppressed by flutamide. Moreover, uptake of benzylpenicillin by TR-BBB cells was also induced by DHT treatment. In contrast, OAT3 mRNA expression in TR-iBRB cells was not affected by DHT treatment. The brain-to-blood efflux rate of benzylpenicillin was not affected by gender. These results suggest that AR is involved in the functional regulation of OAT3 at the BBB, but not at the inner blood-retinal barrier (iBRB), and this regulation is not affected by gender. The BBB function will be affected by the androgen levels in the brain and/or plasma via AR. J. Cell. Physiol. 204: 896–900, 2005. © 2005 Wiley-Liss, Inc.

The blood–brain barrier (BBB) is formed by brain capillary endothelial cells (BCECs) with tight junctions. The BBB expresses various transporters, which act to support and protect the central nervous system (CNS) by supplying nutrients to the brain and excreting metabolites, toxins, and drugs from the brain to blood. Compared with peripheral capillary endothelial cells, BCECs express a variety of unique molecules, such as transporters, receptors, and tight junction proteins (Hosoya et al., 2002), however the molecular mechanisms that induce and maintain the BBB functions in BCECs are still poorly understood.

Gene comparison is one of the most effective strategies for identifying the molecules that are selectively expressed at the BCECs and play unique roles at the BBB. Li and co-workers have reported gene subtraction between rat BCECs, liver and kidney (Li et al., 2002). However, the gene expression in different tissues is too different to allow identification of the molecules controlling the unique functions of the BBB, since the cells in these tissues are a mixture of different type of cells with totally different functions. Therefore, gene comparison should be performed between endothelial cells forming the barrier system in different tissues.

RCECs form the inner blood–retinal barrier (iBRB) by connect with tight junctions as well as BCECs (Cunha-Vaz, 1976). We recently established conditionally immortalized rat BCECs and RCECs (TR-BBB and TR-iBRB, respectively) from transgenic rats harboring a temperature-sensitive SV 40 large T-antigen gene (Hosoya et al., 2000, 2001). TR-BBB and TR-iBRB cells possess endothelial markers and express GLUT1 and P-glycoprotein (Hosoya et al., 2000, 2001), which are expressed at the BBB and inner BRB in vivo as shown by immunohistochemical analysis (Tsuji et al., 1992; Holash and Stewart, 1993; Kumagai, 1999). Thus, TR-BBB and TR-iBRB cells maintain certain in vivo functions, and are a suitable in vitro model for the BBB and iBRB, respectively (Terasaki et al., 2003).

Contract grant sponsor: Japan Society for the Promotion of Science (for Scientific Research and a 21st Century Center of Excellence (COE) Program); Contract grant sponsor: Industrial Technology Research Grant Program of the New Energy and the Industrial Technology Development Organization (NEDO) of Japan.

*Correspondence to: Tetsuya Terasaki, Department of Molecular Biopharmacy and Genetics, Graduate School of Pharmaceutical Sciences, Tohoku University, Aoba, Aramaki, Aoba-ku, Sendai 980-8578, Japan. E-mail: terasaki@mail.pharm.tohoku.ac.jp

Received 12 October 2004; Accepted 4 January 2005

DOI: 10.1002/jcp.20352

The purpose of the present study was to identify selectively expressed genes at the BBB by mRNA differential display analysis of TR-BBB and TR-iBRB cells. The differential display analysis has shown that the androgen receptor (AR) gene is predominantly expressed in TR-BBB cells, and the regulation of transport by AR at the BBB was examined using TR-BBB cells.

MATERIALS AND METHODS

Cell culture

TR-BBB11, TR-BBB13, TR-iBRB2, and TR-iBRB9 cells were established and characterized as described previously (Hosoya et al., 2000, 2001). Cells were seeded onto rat tail collagen type I-coat tissue culture dishes (Becton Dickinson, Bedford, MA). The cells were then cultured in Dulbecco's modified Eagle's medium supplemented with 10% fetal bovine serum (Moregate, Bulimbra, Australia) and 15 μg/l endothelial cell growth factor (Roche Diagnostics, Mannheim, Germany) at 33°C in a humidified atmosphere of 5% CO_2/air. For treatment with DHT or flutamide, the cells were cultured at 33°C with the above medium containing 10 nM DHT (Wako Pure Chemicals, Osaka, Japan) and 0.1% ethanol, or with 10 nM DHT, 1 μM flutamide (Sigma, St. Louis, MO), and 0.1% ethanol. As a control, culture medium containing 0.1% ethanol was used.

mRNA differential display analysis

Differential display was performed using the rhodamine version of a fluorescence differential display kit (Takara, Shiga, Japan) as described previously (Tomi et al., 2004). Briefly, total RNA was prepared from the culture cells using TRIzol reagent (Invitrogen, Carlsbad, CA). After DNase I treatment, RNA was reverse transcribed with a rhodamine labeled arbitrary anchored oligo dT primer. The resulting cDNA was PCR-amplified using the rhodamine labeled arbitrary anchored oligo dT primer and an arbitrary decamer. PCR products were loaded on to 6% polyacrylamide gels, and DNA bands were visualized using a fluorescent image analyzer (FLA3000; Fujifilm, Tokyo, Japan). DNA bands differentially displayed between TR-BBB and TR-iBRB cells were excised from the gel. The eluted DNA was reamplified using the same primer set and PCR conditions. Reamplified PCR products were run on 3% agarose gel containing H.A.-Yellow (Takara) and visualized using the fluorescent image analyzer. The DNA was cloned into a plasmid (pBluescript II SK+; Stratagene, La Jolla, CA), and sequenced using a DNA sequencer (CEQ2000XL; Beckman Coulter, Fullerton, CA). Similarities with other sequences in the GenBank were examined using the BLAST program at the National Center for Biotechnology Information (Bethesda, MD).

RT-PCR analysis

Isolation of the rat brain capillary-rich fraction was performed as described previously (Hosoya et al., 2000). Briefly, cerebrum excised from rats was dissected into pieces, and homogenized in phosphate-buffered saline (PBS). Homogenate was added to the same volume of 32% dextran solution, and then centrifuged (4,500*g*, 20 min, 4°C). The resulting pellets were washed in PBS to obtain the enriched capillary fraction. Total RNA was prepared from the brain capillary-rich fraction using TRIzol reagent (Invitrogen). Reverse-transcription was performed with oligo dT primer. The sequences of the specific primers for AR were as follows: sense, GGTATCCTGGTGGAGTTGTGAACA and antisense, TCACTGTGTGTGGAAATAGATGGGC for rat AR (NM012502; position 2477–3702). PCR was conducted through 35 cycles of 94°C for 30 sec, 55°C for 30 sec, and 72°C for 1 min. The RT-PCR products were separated by electrophoresis on agarose gel. All PCR products were subcloned and sequenced using a DNA sequencer.

Quantitative real-time PCR analysis

Quantitative real-time PCR was performed as described previously (Tomi et al., 2004). Briefly, single-strand cDNA was synthesized from total RNA (1 μg) by reverse transcription using oligo dT primer. According to the manufacturer's protocol, quantitative real-time PCR was performed using an ABI PRISM 7700 sequence detector system (PE-Applied Biosystems) with a 2× SYBR Green PCR master mix (PE-Applied Biosystems), reverse transcribed cDNA, and gene-specific primers. To quantify the amount of target mRNA in the samples, a standard curve was prepared for each run using the plasmid containing the target gene. The mRNA content of organic anion transporter 3 (OAT3) was quantitated within the range of standards, and was standardized by the amount of glyceraldehyde-3-phosphate dehydrogenase (GAPDH). The primer set and amplify condition for AR were the same as that used in RT-PCR analysis. The sequences of the specific primers were as follows: sense, ATCTCATCAACATCTATTGGGT and antisense, CAGAGAGAGACAGAAGGTCA for rat OAT3 (AB017446; position 748–1119); sense, 5′-TGATGACATCAAGAAGGTGGTGAAG-3′ and antisense, 5′-TCCTTGGAGGCCATGTAGGCCAT-3′ for GAPDH (XM217111; position 830–1069). PCR was conducted through 40 cycles of 94°C for 30 sec, 60°C for 1 min, and 72°C for 1 min. The statistical significance of differences among means of several groups was determined by one-way analysis of variance (ANOVA) followed by the modified Fisher's least squares difference method.

Cell uptake study

TR-BBB13 cells (1×10^5 cells/cm^2) were washed with pre-warmed uptake buffer A (135 mM NaCl, 3 mM KCl, 1.4 mM $CaCl_2$, 1.2 mM $MgSO_4$, 0.4 mM K_2HPO_4, 10 mM D-glucose, and 10 mM HEPES, pH 7.4, 290 ± 15 mOsm/kg) at 37°C. The uptake study was initiated at 37°C by applying 200 μl uptake buffer A containing 4.0 μCi [^{3}H]benzylpenicillin (21.0 Ci/mmol, Amersham Biotech, Uppsala, Sweden) and 1.0 μCi [^{14}C]inulin (2.64 Ci/mmol, NEN Life Science, Boston, MA) to estimate the volume of adherent water. After a predetermined interval, cells were washed with ice-cold uptake buffer A and solubilized. Radioactivity was measured in a liquid scintillation counter (LS6500, Beckman-Coulter, Fullerton, CA) and the protein content was determined using a kit (DC, Bio-Rad, Hercules, CA) with bovine serum albumin as a standard. The uptake of [^{3}H]benzylpenicillin was expressed as the cell-to-medium (cell/medium) ratio using the following equation:

$$\text{Cell/medium ratio} = ([^3\text{H}]\ \text{dpm per cell protein (mg)})/([^3\text{H}]\ \text{dpm/μl medium}) - ([^{14}\text{C}]\ \text{dpm per cell protein (mg)})/([^{14}\text{C}]\ \text{dpm/μl medium}).$$

Brain efflux index (BEI) method

The BEI method was performed by the intracerebral microinjection technique as described previously (Kakee et al., 1996). In brief, Wistar rats were anesthetized by intramuscular injection of ketamine-xylazine (1.22 mg xylazine and 125 mg ketamine per kg). Then a freshly prepared solution (0.50 μl), containing 320 nCi [^{14}H]benzylpenicillin and 16 nCi [^{14}C]inulin in an extracellular fluid buffer (122 mM NaCl, 25 mM $NaHCO_3$, 3 mM KCl, 1.4 mM $CaCl_2$, 1.2 mM $MgSO_4$, 0.4 mM K_2HPO_4, 10 mM D-glucose, and 10 mM HEPES, pH 7.4), was administered into the Parietal Cortex Area 2 region over a period of 1 min. At designated times (2, 20, and 40 min), the whole brain was removed and the left cerebrum, right cerebrum, and cerebellum were isolated. Brain samples were solubilized and mixed with Hionic-fluor (Packard, Meriden, CT). The radioactivity remaining in the brain was measured in a liquid scintillation counter. The percentage of substrate remaining in the ipsilateral cerebrum (100-BEI) was determined from following equation:

$$100\text{-BEI}\ (\%) = [(\text{amount of test substrate in the brain})/(\text{amount of reference in the brain})]/[(\text{concentration of test substrate injected})/(\text{concentration of reference injected})] \times 100.$$

The apparent brain efflux rate constant (k_{eff}) across the BBB was estimated from the slope given by fitting a semilogarithmic plot of (100-BEI), that is, the concentration remaining in the

TABLE 1. Genes dominantly expressed in TR-BBB cells

No.	Length (bp)	mRNA ratio	Highest homology genes	Identity
1	287	1,730	Mouse androgen receptor, 3′-UTR	91/91 (100%)
2	389	16.9	Mouse clone RP23-443D3 (Chr2)	80/88 (90%)
3	95	8.08	Mouse clone RP23-47J12 (Chr11)	70/75 (93%)
4	375	6.88	Mouse clone RP23-60i12 (Chr2)	113/133 (84%)
5	92	4.52	Mouse hypothetical protein LOC217831	81/86 (94%)
6	136	3.32	Rat BAC CH230-9H16	57/61 (93%)
7	194	2.99	Rat hypothetical protein LOC309523	152/153 (99%)
8	300	2.96	Rat BAC CH230-24G20	298/298 (100%)
9	204	2.75	Mouse clone IMAGE:5354131	163/181 (90%)
10	391	2.47	Mouse clone RP23-445E3 (Chr4)	134/165 (81%)
11	284	2.43	Mouse cDNA clone:6030408G03	195/220 (88%)
12	112	2.26	Mouse clone RP24-75F14 (Chr1)	98/111 (88%)

The mRNA ratio is the ratio of the mRNA level in TR-BBB cells to that in TR-iBRB cells normalized by the mRNA level of GAPDH. Identity indicates the number of identical nucleotide versus the number of nucleotide in the identical region.

ipsilateral cerebrum versus time, using nonlinear least-squares regression analysis.

RESULTS

Differential display between TR-BBB and TR-iBRB cells

The differential display analysis of TR-BBB11, TR-BBB13, TR-iBRB2, and TR-iBRB9 cells showed a number of DNA bands selectively expressed in TR-BBB cells. The DNA bands of 100 ~ 450 bp were cloned and sequenced. Quantitative real-time PCR using specific primers for each clone was performed to confirm the reproducibility. As a result of these analyses, 12 clones were identified and found to be expressed to a greater extent in TR-BBB cells than in TR-iBRB cells (Table 1). Clone 1 of 287 bp, which was expressed 1730-fold more intensely in TR-BBB cells than in TR-iBRB cells, exhibited the largest difference in mRNA expression level of the 12 clones. A portion of the sequence of clone 1 exhibited 100% and 99% nucleotide identity with the 3′-UTR of the mouse and human AR (99/99 and 120/121), respectively.

Dominant expression of AR in rat BCECs

The expression of rat AR mRNA was examined by RT-PCR analysis amplifying the coding region of rat AR (Fig. 1). A band was detected in TR-BBB11, TR-BBB13 cells, and brain capillary-rich fraction at the expected size, while no band was detected in TR-iBRB2 and TR-iBRB9 cells. The expression of AR mRNA was quantified by means of real-time RT-PCR standardized by that of GAPDH mRNA, and the expression of AR mRNA in TR-BBB cells is 3,400-fold higher than that in TR-iBRB cells. The sequence of the amplified product was identical to that of rat AR.

Induction of OAT3 expression by AR

OAT3 is a transporter expressed at the BBB, and its expression in males has been reported to be greater than that in females as far as the liver and kidney are concerned (Kobayashi et al., 2002; Ljubojevic et al., 2004). Therefore, the regulation of OAT3 mRNA expression by AR was investigated (Fig. 2). The mRNA expression of AR was normalized by that of GAPDH, and the expression levels of GAPDH mRNA in the cells varied less than twofold in this experiment (data not shown). TR-BBB13 cells were treated with dihydrotestosterone (DHT), an AR ligand. At 9 and 12 h after treatment, OAT3 mRNA expression was induced 1.65- and 1.95-fold, respectively, compared with the untreated cells. This induction was almost completely suppressed by flutamide, an AR inhibitor. In contrast, no induction of OAT3 mRNA by DHT was detected in TR-iBRB2 cells.

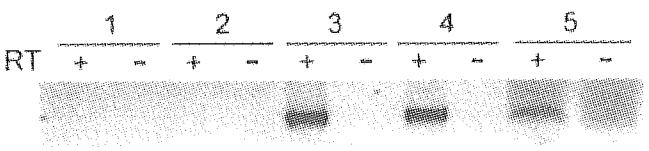

Fig. 1. Selective mRNA expression of rat AR in TR-BBB cells and the brain capillary-rich fraction. An amplified band was detected at 1018 bp. (1) TR-iBRB2 cells; (2) TR-iBRB9 cells; (3) TR-BBB11 cells; (4) TR-BBB13 cells; (5) rat brain capillary-rich fraction. Reactions were performed against total RNA with (+) or without (−) reverse transcription (RT).

Induction of OAT3 function by AR

The transport function of OAT3 was evaluated by cellular uptake using [^{3}H]benzylpenicillin, a specific substrate for OAT3. [^{3}H]Benzylpenicillin uptake by TR-BBB13 cells increased linearly for at least 10 min (Fig. 3), and so the transport function of OAT3 was evaluated at 5 min.

After DHT treatment for less than 24 h, no difference in [^{3}H]benzylpenicillin uptake was detected between DHT-treated and control cells (Fig. 4). After treatment for 36 and 72 h, the uptake increased by 1.56- and 1.67-fold compared with control cells, respectively (Fig. 4). This result suggests that the transport function of OAT3 is induced by DHT.

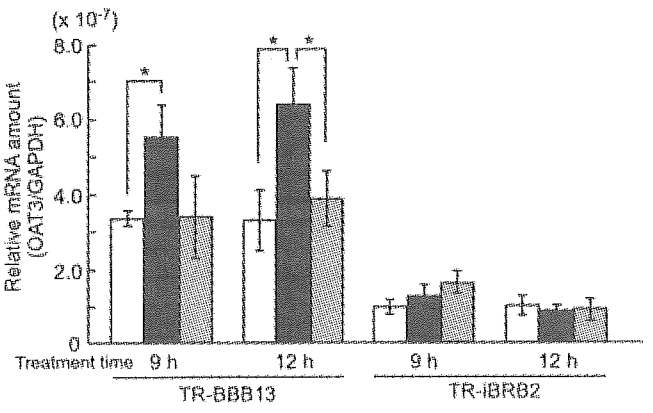

Fig. 2. Effect of DHT and flutamide on mRNA levels of rat OAT3 in TR-BBB13 and TR-iBRB2 cells. TR-BBB13 and TR-iBRB2 cells were treated with culture medium containing either 10 nM DHT (■) or 10nM DHT and 1 μM flutamide (▨), or control medium (□). mRNA levels of OAT3 were normalized by the mRNA levels of GAPDH. Each bar represents the mean ± SEM (n = 3–6). *$P < 0.05$, significant difference.

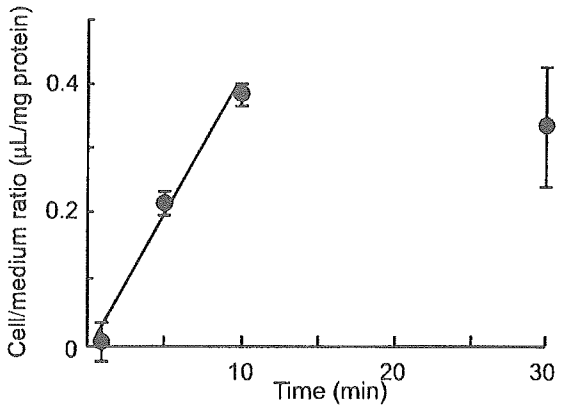

Fig. 3. Uptake of [^{3}H]benzylpenicillin by TR-BBB13 cells. The uptake of [^{3}H]benzylpenicillin was measured at 1, 5, 10, and 30 min. The uptake was expressed as the cell-to-medium (cell/medium) ratio. The initial uptake, which was estimated by least-squares regression, is indicated as a line. The initial uptake rate was calculated to be 4.21×10^{-2} μl/(mg protein × min). Each point represents the mean ± SEM (n = 4).

Effect of gender on OAT3-mediated efflux transport at the BBB

To investigate the effect of gender on OAT3 function at the in vivo BBB, the brain-to-blood efflux transport of [^{3}H]benzylpenicillin was examined by the BEI method. The efflux rates of male and female animals were found to be $5.57 \times 10^{-2} \pm 0.52 \times 10^{-2}$/min and $6.46 \times 10^{-2} \pm 0.46 \times 10^{-2}$/min (mean ± SEM, n = 3), respectively, and there was no significant difference between the efflux rate of males and females.

DISCUSSION

In this study, 12 gene clones were identified as highly expressed genes in rat BCECs (TR-BBB cells) compared with RCECs (TR-iBRB cells) by mRNA differential display analysis (Table 1). Using these culture cells overcame the problems posed by contamination by non-endothelial cells and the limited size of the organs. In addition, TR-BBB and TR-iBRB cells were established from the same strain of male transgenic rat, harboring temperature sensitive SV40 large T antigen gene, of the same age by using a similar procedure, which did not involve gene transfection (Terasaki et al., 2003). Therefore, the difference in expressed genes between these cell lines did indeed reflect the difference between the BBB and iBRB in vivo.

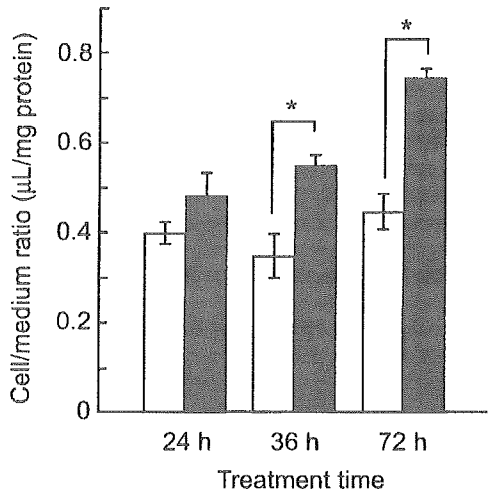

Fig. 4. Effect of DHT on the uptake of benzylpenicillin by TR-BBB cells. TR-BBB cells were cultured in the presence (■) or absence (control, □) of 10 nM DHT. The uptake was measured at 5 min. Each bar represents the mean ± SEM (n = 4). *$P < 0.05$, significantly different from control.

The function of the identified BBB dominant genes, except clone 1, is unknown, since these gene fragments have the highest homology with functionally unknown genes (Table 1). The BBB dominant expression of these genes might provide helpful information for further studies of their gene function. The differential display using TR-BBB and TR-iBRB cells could also be used to identify the iBRB dominant gene. We have already reported that M-cadherin, GATA-binding protein-3, and cytosolic branched chain amino transferase are more abundantly expressed in TR-iBRB cells than TR-BBB cells and may be involved in unique functions at the iBRB (Tomi et al., 2004).

AR is a nuclear receptor regulating gene expression by binding to androgens (Santos et al., 2004). The most selective gene fragment in TR-BBB cells has a high degree of homology with the 3′-UTR of mouse and human AR. The nucleotide sequence of rat AR cDNA including 3′-UTR has been reported (Chang et al., 1988), whereas a sequence similar to that of the identified gene fragment was not found in the reported rat AR cDNA. Human AR has been reported to have splicing variants, which have different lengths of 3′-UTR (Faber et al., 1991). Therefore, the reported rat AR cDNA would be a splicing variant lacking the region of the identified fragment. Following RT-PCR analysis of the coding region, AR mRNA was found to be expressed in TR-BBB cells and the brain capillary rich-fraction, but not in TR-iBRB cells (Fig. 1). This result suggests selective mRNA expression of AR at the BBB.

Gene and functional induction by DHT, an AR ligand, was detected in TR-BBB13 cells, and this induction was suppressed by flutamide (Fig. 2). Although estrogens, which are produced from androgens by aromatase, are able to induce gene expression by interaction with estrogen receptors (Allolio and Arlt, 2002), the inhibition of flutamide indicates that the induction of OAT3 expression and function by DHT resulted from an interaction between DHT and AR. In contrast, no gene induction by DHT was detected in TR-iBRB cells (Fig. 2). These results suggest that an AR-mediating gene regulation exists at the BBB but not at the iBRB. In the non-treated conditions, OAT3 expression in TR-BBB cells is greater than that in TR-iBRB cells (3.3-fold at 12 h treatment). This suggests that the OAT3 was basally induced in TR-BBB cells.

Gene induction of OAT3 was detected after 9 h of DHT treatment, while significant functional induction of OAT3 was detected after 36 h of the treatment. The functional delay of transporters has also been detected in the induction of system A in TR-BBB cells under hypertonic conditions (Takanaga et al., 2002). This functional delay could be attributed to the transcription from mRNA, molecular modification, and translocation to the plasma membrane.

The present study is the first demonstration of the AR-mediated regulation of OAT3 function at the BBB. Male dominant expression of OAT3 has been reported in rat liver and kidney (Kobayashi et al., 2002; Ljubojevic et al., 2004). These reports have also shown that OAT3 expression in the liver and kidney was reduced in castrated male rats, and this reduction was reversed by testosterone treatment, but not by estradiol treatment. Searching the upstream region of rat OAT3, the sequence, which is similar to the high-affinity AR

specific androgen response element in rat probasin promoter (5′-GGTTCTtgcAGTACT-3′) (Claessens et al., 1996), is located 1 kbp upstream from the potent transcription start site (−1126: 5′-GGTAATcctAGTACT-3′: −1112). Therefore, it is conceivable that the induction of OAT3 gene is mediated by the interaction of AR and the *cis*-response element on the OAT3 promoter.

The BCECs face the circulating blood and also the brain parenchyma. Sex hormones exist in the brain, and the brain level of dehydroepiandrosterone (DHEA) is about fourfold higher than that in plasma (Corpechot et al., 1981; Hojo et al., 2004). Therefore, it is likely that androgen signals from the brain control the AR mediating gene regulation rather than those from the circulating blood. Indeed, no gender difference was detected in the brain-to-blood efflux rate of benzylpenicillin, an OAT3 selective substrate, in adult rats. The possibility that the contribution of other regulatory mechanism(s) also plays a role in maintaining OAT3 function at the BBB cannot be ruled out or that the limiting process in the efflux transport of benzylpenicillin is luminal efflux transport and not abluminal uptake by OAT3, the dominant regulation from the brain side agrees with the physiological function of OAT3 at the BBB. Because OAT3 is the transporter responsible for the brain-to-blood efflux of dopamine metabolites, such as homovanillic acid, uremic toxins, and drugs (Ohtsuki et al., 2002, 2004; Mori et al., 2003, 2004). If OAT3 expression is influenced by the plasma levels of androgens, which exhibit gender and diurnal variations, the BBB will be unable to maintain a constant CNS milieu.

In conclusion, the present study describes a comparison of gene expression between the rat BBB and iBRB, and the identification of 12 BBB dominant genes. AR, which is the most selective BBB gene, regulates the expression and function of OAT3 at the BBB. These results suggest that the comparison of gene expression is one of the most effective strategies for identifying novel barrier functions and regulation systems. In addition, the further analysis of the genes regulated by AR at the BBB will play an important role in increasing our understanding of the physiological function of the AR at the BBB and the effects of sex hormones on BBB functions under physiological and pathological conditions.

ACKNOWLEDGMENTS

We thank Ms. N. Funayama for secretarial assistance.

LITERATURE CITED

Allolio B, Arlt W. 2002. DHEA treatment: Myth or reality? Trends Endocrinol Metab 13(7):288–294.

Chang CS, Kokontis J, Liao ST. 1988. Structural analysis of complementary DNA and amino acid sequences of human and rat androgen receptors. Proc Natl Acad Sci USA 85(19):7211–7215.

Claessens F, Alen P, Devos A, Peeters B, Verhoeven G, Rombauts W. 1996. The androgen-specific probasin response element 2 interacts differentially with androgen and glucocorticoid receptors. J Biol Chem 271(32):19013–19016.

Corpechot C, Robel P, Axelson M, Sjovall J, Baulieu EE. 1981. Characterization and measurement of dehydroepiandrosterone sulfate in rat brain. Proc Natl Acad Sci USA 78(8):4704–4707.

Cunha-Vaz JG. 1976. The blood-retinal barriers. Doc Ophthalmol 41(2):287–327.

Faber PW, van Rooij HC, van der Korput HA, Baarends WM, Brinkmann AO, Grootegoed JA, Trapman J. 1991. Characterization of the human androgen receptor transcription unit. J Biol Chem 266(17):10743–10749.

Hojo Y, Hattori TA, Enami T, Furukawa A, Suzuki K, Ishii HT, Mukai H, Morrison JH, Janssen WG, Kominami S, Harada N, Kimoto T, Kawato S. 2004. Adult male rat hippocampus synthesizes estradiol from pregnenolone by cytochromes P45017alpha and P450 aromatase localized in neurons. Proc Natl Acad Sci USA 101(3):865–870.

Holash JA, Stewart PA. 1993. The relationship of astrocyte-like cells to the vessels that contribute to the blood-ocular barriers. Brain Res 629(2):218–224.

Hosoya K, Takashima T, Tetsuka K, Nagura T, Ohtsuki S, Takanaga H, Ueda M, Yanai N, Obinata M, Terasaki T. 2000. mRNA expression and transport characterization of conditionally immortalized rat brain capillary endothelial cell lines; a new in vitro BBB model for drug targeting. J Drug Target 8(6):357–370.

Hosoya K, Tomi M, Ohtsuki S, Takanaga H, Ueda M, Yanai N, Obinata M, Terasaki T. 2001. Conditionally immortalized retinal capillary endothelial cell lines (TR-iBRB) expressing differentiated endothelial cell functions derived from a transgenic rat. Exp Eye Res 72(2):163–172.

Hosoya K, Ohtsuki S, Terasaki T. 2002. Recent advances in the brain-to-blood efflux transport across the blood-brain barrier. Int J Pharm 248(1–2):15–29.

Kakee A, Terasaki T, Sugiyama Y. 1996. Brain efflux index as a novel method of analyzing efflux transport at the blood-brain barrier. J Pharmacol Exp Ther 277(3):1550–1559.

Kobayashi Y, Hirokawa N, Ohshiro N, Sekine T, Sasaki T, Tokuyama S, Endou H, Yamamoto T. 2002. Differential gene expression of organic anion transporters in male and female rats. Biochem Biophys Res Commun 290(1):482–487.

Kumagai AK. 1999. Glucose transport in brain and retina: Implications in the management and complications of diabetes. Diabetes Metab Res Rev 15(4):261–273.

Li JY, Boado RJ, Pardridge WM. 2002. Rat blood-brain barrier genomics II. J Cereb Blood Flow Metab 22(11):1319–1326.

Ljubojevic M, Herak-Kramberger CM, Hagos Y, Bahn A, Endou H, Burckhardt G, Sabolic I. 2004. Rat renal cortical OAT1 and OAT3 exhibit gender differences determined by both androgen stimulation and estrogen inhibition. Am J Physiol Renal Physiol 287(1):F124–F138.

Mori S, Takanaga H, Ohtsuki S, Deguchi T, Kang YS, Hosoya K, Terasaki T. 2003. Rat organic anion transporter 3 (rOAT3) is responsible for brain-to-blood efflux of homovanillic acid at the abluminal membrane of brain capillary endothelial cells. J Cereb Blood Flow Metab 23(4):432–440.

Mori S, Ohtsuki S, Takanaga H, Kikkawa T, Kang YS, Terasaki T. 2004. Organic anion transporter 3 is involved in the brain-to-blood efflux transport of thiopurine nucleobase analogs. J Neurochem 90(4):931–941.

Ohtsuki S, Asaba H, Takanaga H, Deguchi T, Hosoya K, Otagiri M, Terasaki T. 2002. Role of blood-brain barrier organic anion transporter 3 (OAT3) in the efflux of indoxyl sulfate, a uremic toxin: Its involvement in neurotransmitter metabolite clearance from the brain. J Neurochem 83(1):57–66.

Ohtsuki S, Kikkawa T, Mori S, Hori S, Takanaga H, Otagiri M, Terasaki T. 2004. Mouse reduced in osteosclerosis transporter functions as an organic anion transporter 3 and is localized at abluminal membrane of blood-brain barrier. J Pharmacol Exp Ther 309(3):1273–1281.

Santos AF, Huang H, Tindall DJ. 2004. The androgen receptor: A potential target for therapy of prostate cancer. Steroids 69(2):79–85.

Takanaga H, Tokuda N, Ohtsuki S, Hosoya K, Terasaki T. 2002. ATA2 is predominantly expressed as system A at the blood-brain barrier and acts as brain-to-blood efflux transport for L-proline. Mol Pharmacol 61(6):1289–1296.

Terasaki T, Ohtsuki S, Hori S, Takanaga H, Nakashima E, Hosoya K. 2003. New approaches to in vitro models of blood-brain barrier drug transport. Drug Discov Today 8(20):944–954.

Tomi M, Abukawa H, Nagai Y, Hata T, Takanaga H, Ohtsuki S, Terasaki T, Hosoya K. 2004. Retinal selectivity of gene expression in rat retinal versus brain capillary endothelial cell lines by differential display analysis. Mol Vis 10:537–543.

Tsuji A, Terasaki T, Takabatake Y, Tenda Y, Tamai I, Yamashima T, Moritani S, Tsuruo T, Yamashita J. 1992. P-glycoprotein as the drug efflux pump in primary cultured bovine brain capillary endothelial cells. Life Sci 51(18):1427–1437.

Impact of the Liver-Specific Expression of SHIP2 (SH2-Containing Inositol 5′-Phosphatase 2) on Insulin Signaling and Glucose Metabolism in Mice

Kazuhito Fukui,[1] Tsutomu Wada,[1] Syota Kagawa,[2] Kiyofumi Nagira,[1] Mariko Ikubo,[1] Hajime Ishihara,[3] Masashi Kobayashi,[1] and Toshiyasu Sasaoka[2]

We investigated the role of hepatic SH2-containing inositol 5′-phosphatase 2 (SHIP2) in glucose metabolism in mice. Adenoviral vectors encoding wild-type SHIP2 (WT-SHIP2) and a dominant-negative SHIP2 (ΔIP-SHIP2) were injected via the tail vein into db/+m and *db/db* mice, respectively. Four days later, amounts of hepatic SHIP2 protein were increased by fivefold. Insulin-induced phosphorylation of Akt in liver was impaired in WT-SHIP2–expressing db/+m mice, whereas the reduced phosphorylation was restored in ΔIP-SHIP2–expressing *db/db* mice. The abundance of mRNA for glucose-6-phosphatase (G6Pase) and PEPCK was increased, that for glucokinase (GK) was unchanged, and that for sterol regulatory element–binding protein 1 (SREBP)-1 was decreased in hepatic WT-SHIP2–overexpressing db/+m mice. The increased expression of mRNA for G6Pase and PEPCK was partly suppressed, that for GK was further enhanced, and that for SREBP1 was unaltered by the expression of ΔIP-SHIP2 in *db/db* mice. The hepatic expression did not affect insulin signaling in skeletal muscle and fat tissue in both mice. After oral glucose intake, blood glucose levels and plasma insulin concentrations were elevated in WT-SHIP2–expressing db/+m mice, while elevated values were decreased by the expression of ΔIP-SHIP2 in *db/db* mice. These results indicate that hepatic SHIP2 has an impact in vivo on the glucose metabolism in both physiological and diabetic states possibly by regulating hepatic gene expression. *Diabetes* 54:1958–1967, 2005

From the [1]First Department of Internal Medicine, Toyama Medical & Pharmaceutical University, Toyama, Japan; the [2]Department of Clinical Pharmacology, Toyama Medical & Pharmaceutical University, Toyama, Japan; and [3]Sainou Hospital, Toyama, Japan.

Address correspondence and reprint requests to Toshiyasu Sasaoka, MD, PhD, Department of Clinical Pharmacology, Toyama Medical & Pharmaceutical University, 2630 Sugitani, Toyama, 930-0194, Japan. E-mail: tsasaoka-tym@umin.ac.jp.

Received for publication 15 November 2004 and accepted in revised form 11 April 2005.

G6Pase, glucose-6-phosphatase; GK, glucokinase; ΔIP-SHIP2, dominant-negative SHIP2; IRS, insulin receptor substrate; PI, phosphatidylinositol; PTEN, 3′-lipid phosphatase; SHIP2, SH2-containing inositol 5′-phosphatase 2; SREBP, sterol regulatory element–binding protein; WT-SHIP2, wild-type SHIP2.

Insulin binding to the insulin receptor in turn phosphorylates insulin receptor substrates (IRSs) at tyrosine residues (1,2). The tyrosine-phosphorylated IRS binds to the p85 regulatory subunit of phosphatidylinositol (PI) 3-kinase, resulting in the activation of the p110 subunit (3,4). PI 3-kinase functions as a lipid kinase to produce $PI(3,4,5)P_3$ from $PI(4,5)P_2$ in vivo (5). $PI(3,4,5)P_3$ is crucial as a lipid second messenger in various metabolic effects of insulin (3,6–8). $PI(3,4,5)P_3$ mediates insulin signals to downstream molecules including Akt (9). Akt is the key signaling molecule in the activation of glucose uptake in the skeletal muscle and fat tissue and in the regulation of mRNA expression for gluconeogenesis, glycolysis, and lipid synthesis in the liver (10). SH2-containing inositol 5′-phosphatase 2 (SHIP2) was identified as a lipid phosphatase that hydrolyzes $PI(3,4,5)P_3$ to $PI(3,4)P_2$ (11,12). Targeted disruption of the SHIP2 gene in mice caused an increase in insulin sensitivity without affecting other biological systems (13). In addition, some polymorphisms of the SHIP2 gene found in British and French populations are associated with metabolic syndromes including type 2 diabetes and hypertension (14). The expression of SHIP2 could be elevated in type 2 diabetic subjects with a 16-bp deletion in the 3′-untranslated regulatory region of the SHIP2 gene (15). Based on these reports, SHIP2 appears to be a physiologically important negative regulator relatively specific to insulin signaling with an impact on the state of insulin resistance (13–17).

We have previously reported that overexpression of SHIP2, via 5′-phosphatase activity, impaired insulin-induced activation of Akt resulting in decreased glucose uptake and glycogen synthesis in 3T3-L1 adipocytes and L6 myocytes (18,19). Although we clarified the role and molecular mechanisms by which SHIP2 regulates insulin signaling in the skeletal muscle and fat tissue (20–22), the impact of SHIP2 in the liver on the metabolism of glucose in vivo is largely unknown. Based on studies with tissue-specific knockout of the insulin receptor in mice, the liver was found to be the most critical target tissue of insulin action in the control of glucose homeostasis (23,24). Insulin regulates hepatic glucose output through suppression of hepatic gluconeogenic gene expression via the IRS-2/PI 3-kinase pathway and augmentation of glycolytic gene expression via the IRS-1/PI 3-kinase pathway (25–30).

Sterol regulatory element–binding protein (SREBP)-1c is the key factor involved in insulin resistance by controlling lipid synthesis via the IRS-1/PI 3-kinase pathway (30). On the basis of these results, it is possible that SHIP2 in the liver functions as a negative regulator of the PI 3-kinase–dependent metabolic action of insulin. Therefore, it would be of particular importance to clarify the impact of hepatic SHIP2 on the regulation of insulin signaling and hepatic gene expression for the control of glucose homeostasis in diabetic model mice as well as in nondiabetic mice.

In the present study, we investigated the impact of liver-specific overexpression of SHIP2 in lean db/+m mice and liver-specific inhibition of SHIP2 in diabetic *db/db* mice. Adenoviral vectors encoding wild-type SHIP2 (WT-SHIP2) and the dominant-negative mutant of SHIP2 (ΔIP-SHIP2) were injected, via the tail vein, into the db/+m and *db/db* mice, respectively. We studied the effect of hepatic SHIP2 expression on insulin signaling leading to hepatic gene expression. In addition, we examined whether the liver-specific expression of SHIP2 affects the metabolic actions of insulin in skeletal muscle and fat tissue. Furthermore, glucose metabolism was investigated by conducting glucose tolerance tests and insulin tolerance tests in WT-SHIP2–expressing db/+m and ΔIP-SHIP2–expressing *db/db* mice.

RESEARCH DESIGN AND METHODS

Human regular insulin HumalinR was provided by Eli Lilly. A polyclonal anti–IRS-1 antibody and a polyclonal anti-Thr^{308} phospho-specific Akt antibody were purchased from Cell Signaling Technology (Beverly, MA). A polyclonal anti–IRS-2 antibody and a polyclonal anti-Ser^{473} phospho-specific Akt antibody were obtained from Upstate Biotechnology (Lake Placid, NY). A polyclonal anti-Akt antibody was purchased from Santa Cruz Biotechnology (Santa Cruz, CA). A monoclonal anti-phosphotyrosine antibody (PY99) was purchased from Transduction Laboratories (Lexington, KY). The polyclonal anti-SHIP2 antibody has been described previously (12). Enhanced chemiluminescence reagents were obtained from Amersham Pharmacia Biotech (Uppsala, Sweden). All other routine reagents were of analytical grade and purchased from Sigma Chemicals (St. Louis, MO) or Wako Pure Chemical Industries (Osaka, Japan).

Male C57BL/KsJ-*db/db* Jcl (BKS.Cg-+*Lepr^{db}*/+*Lepr^{db}*/Jcl) mice, their lean heterozygote littermates (*db/+m*), and C57BL/6J mice were purchased from Clea Japan (Tokyo, Japan) at 6 weeks of age. Mice were maintained under standard light (12 h light/dark) and temperature conditions. These mice were caged in groups of four and were provided with standard rodent diet and water ad libitum.

Adenovirus-mediated gene transfer in the liver. Adenoviral vectors encoding rat WT-SHIP2 and a PI 5′-phosphatase–defective ΔIP-SHIP2 have been described previously (18). Eight-week-old male mice were injected with the adenovirus via the tail vein at a concentration of 5×10^8 pfu (plaque-forming units)/g body wt in a suspension of 200 μl PBS. Experiments were performed 4 days after the injection. All procedures were approved by the Committee of Animal Experiments at Toyama Medical & Pharmaceutical University.

Western blot analysis. Mice deprived of food for 16 h were injected with human regular insulin (5 units/kg body wt) or saline via the tail vein. After 5 min, the mice were anesthetized and killed to isolate the liver, hindlimb muscle, and epididymal fat. These tissues were homogenized using a polytron at half-maximal speed (15,000 rpm) for 1 min on ice in 500 μl of a homogenization buffer containing 20 mmol/l Tris, 5 mmol/l EDTA, 10 mmol/l $Na_4P_2O_7$, 100 mmol/l NaF, 2 mmol/l Na_3VO_4, 1% NP-40, 1 mmol/l phenylmethylsulfonyl fluoride, 10 μg/ml aprotinin, and 10 μg/ml leupeptin (pH 7.5). The tissue lysates were solubilized by continuous stirring for 1 h at 4°C and centrifuged for 30 min at 14,000*g*. The supernatants (200 μg protein) were immunoprecipitated with indicated antibodies for 2 h at 4°C. The precipitates or the lysates were separated by 7.5% SDS-PAGE and transferred onto polyvinylidene difluoride membranes using a Bio-Rad Transblot apparatus. The membranes were blocked in a buffer containing 50 mmol/l Tris, 150 mmol/l NaCl, 0.1% Tween 20, and 5% nonfat milk (pH 7.5) for 2 h at 20°C. They were then probed with antibodies for 16 h at 4°C. After the membranes had been washed in a buffer containing 50 mmol/l Tris, 150 mmol/l NaCl, and 0.1% Tween 20 (pH 7.5), blots were incubated with horseradish peroxidase–linked second antibody and then examined by enhanced chemiluminescence (ECL) detection using an ECL reagent according to the manufacturer's instructions (Amersham). In each experiment, the intensity of the band derived from insulin-induced phosphorylation of IRS-1, IRS-2, and Akt in control db/+m mice was assigned as a value of 1 arbitrary unit, and the intensity of all treated groups in *db/db* mice was expressed as a fold value of control.

Northern blot analysis. Mice deprived of food for 16 h were anesthetized and killed, and the liver was removed and frozen in liquid N2. Mice were not fasted for the analysis of SREBP1 mRNA. Total RNA was extracted from 50 mg of the liver sample using the QuickPrep total RNA Extraction Kit (Amersham). Total RNA (10 μg) for each sample was separated using a 1% agarose gel and transferred to a Hybond-H$^+$ positively charged nylon membrane (Amersham). Probes for glucokinase (GK) (31), SREBP-1 (32), PEPCK (33), glucose-6-phosphatase (G6Pase) (34), and Glut2 (35) mRNAs were kindly provided by T. Noguchi (Nagoya University, Nagoya, Japan), H. Shimano (Tsukuba University, Ibaragi, Japan), D.K. Granner (Vanderbilt University Medical Center, Nashville, TN), H. Nakajima (Osaka Medical Center for Cancer and Cardiovascular Disease, Osaka, Japan), and W. Ogawa (Kobe University, Kobe, Japan), respectively. Each probe was chemiluminescently labeled and hybridized, and the mRNA expression was detected using the AlkPhos Direct Labeling and Detection System with CDP-Star (Amersham Biosciences).

Oral glucose tolerance test and insulin tolerance test. For the oral glucose tolerance test, mice deprived of food for 16 h were loaded orally with glucose (2 g/kg). Blood samples were collected from the orbital sinus at various time points after the loading. For the insulin tolerance test, mice deprived of food for 8 h were injected intraperitoneally with human regular insulin (0.75 units/kg). Blood samples were collected from the tail vein at various time points. Blood glucose levels were then measured with a FreeStyle KISSEI (Kissei, Japan), and blood insulin concentrations were measured with an enzyme-linked immunosorbent assay kit (Morinaga, Japan).

Statistical analysis. Data are presented as means ± SE. P values were determined using a paired t test or Bonferroni test with ANOVA. $P < 0.05$ was considered statistically significant.

RESULTS

Expression of SHIP2 in the liver of mice injected with an adenoviral vector via the tail vein. Systemic adenoviral injection into mice via the tail vein is known to result in the liver-specific expression of the exogenous gene (36). The 5′-phosphatase–defective ΔIP-SHIP2 acts as a dominant-negative mutant possibly by competing with endogenous SHIP2 to bind PI(3,4,5)P_3 (18). By inhibiting the endogenous function of SHIP2, ΔIP-SHIP2 augments insulin signaling mediated by the PI 3-kinase product PI(3,4,5)P_3 (18,19). Hepatic expression of both WT-SHIP2 and ΔIP-SHIP2 was detected 1 day after the adenoviral injection. The abundance was maximal at 4 days, decreased thereafter, and returned to the basal level at 14 days after the injection (data not shown). Therefore, we examined the expression of WT-SHIP2 and ΔIP-SHIP2 in various tissues of mice 4 days after the adenoviral injection. As shown in Fig. 1, we observed fivefold greater amounts of exogenous WT-SHIP2 and ΔIP-SHIP2 than endogenous SHIP2 in the liver. The lower band seen in the liver of mice may be a splicing variant of SHIP2. Alternatively, we cannot rule out the possibility that the band originated from the degradation of SHIP2 during the preparation of samples. Except for the liver, expression of either exogenous WT-SHIP2 or ΔIP-SHIP2 was not detectable in the various tissues examined. The body weight of the mice was not changed by the liver-specific expression of SHIP2 (data not shown). We analyzed the effect of liver-specific expression of WT-SHIP2 in control db/+m mice and ΔIP-SHIP2 in diabetic *db/db* mice on the metabolic action of insulin.

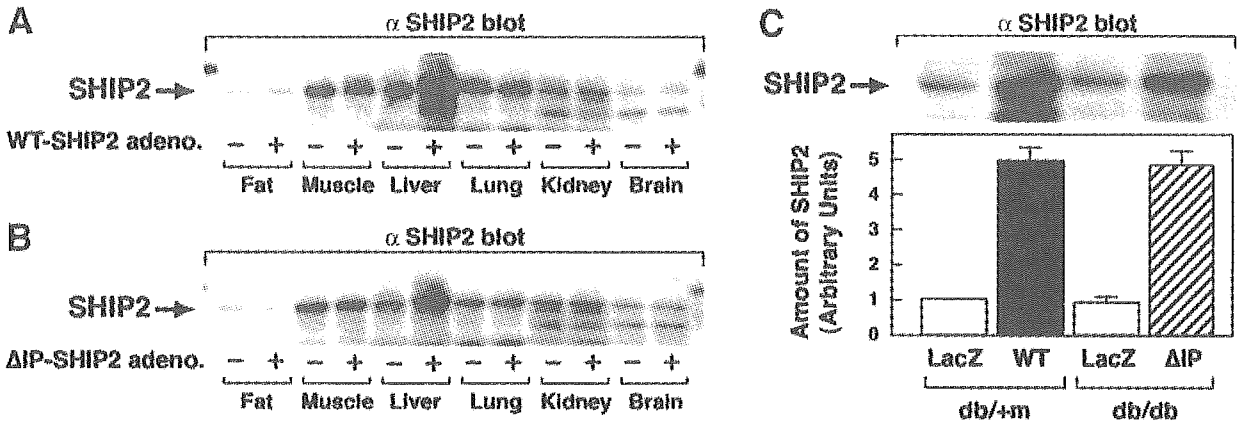

FIG. 1. Expression of SHIP2 in the liver of mice injected with an adenoviral vector via the tail vein. Total homogenates of the indicated tissues obtained from db/+m and *db/db* mice 4 days after adenoviral injection with WT-SHIP2 (*A*) and ΔIP-SHIP2 (*B*), respectively, were subjected to immunoblot analysis with anti-SHIP2 antibody. The amount of SHIP2 in the liver is shown as means ± SE of three separate experiments (*C*).

Effect of WT-SHIP2 expression on insulin-induced phosphorylation of IRS and Akt in the liver of db/+m mice. Mice injected with the adenoviral vector encoding WT-SHIP2 or control LacZ were deprived of food for 16 h and then injected intravenously with insulin (5 units/kg) or saline (200 μl) for 5 min. Thereafter, the liver was removed and subjected to immunoblot analysis (Fig. 2). Amounts of IRS-1, IRS-2, and Akt were not altered by expression of WT-SHIP2 in the liver of db/+m mice (Fig. 2*A*–*C*). Insulin-induced tyrosine phosphorylation of IRS-1 and IRS-2 was also comparable between WT-SHIP2– and LacZ-injected db/+m mice (Figs. 2*A* and *B*). Akt is a crucial mediator of IRS/PI 3-kinase signaling and is known to be activated by phosphorylation at Thr^{308} and Ser^{473} residues (10,37,38). Insulin induced phosphorylation of Akt at Thr^{308} in the liver of LacZ-transfected db/+m mice. The extent of the phosphorylation was decreased by 49.0 ± 13.0% in the liver of WT-SHIP2–overexpressing db/+m mice (Fig. 2*C*). Similar results were obtained in C57BL/6J mice (data not shown).

Effect of ΔIP-SHIP2 expression on insulin-induced phosphorylation of IRS and Akt in the liver of *db/db* mice. We next examined the ameliorative effect of the liver-specific expression of ΔIP-SHIP2 on the metabolic signaling of insulin in the liver of diabetic *db/db* mice (Fig. 3). In *db/db* mice, the amount of IRS-1 and IRS-2 was decreased by 27.9 ± 4.8 and 73.6 ± 5.2%, respectively, compared with db/+m mice, whereas the amount of Akt

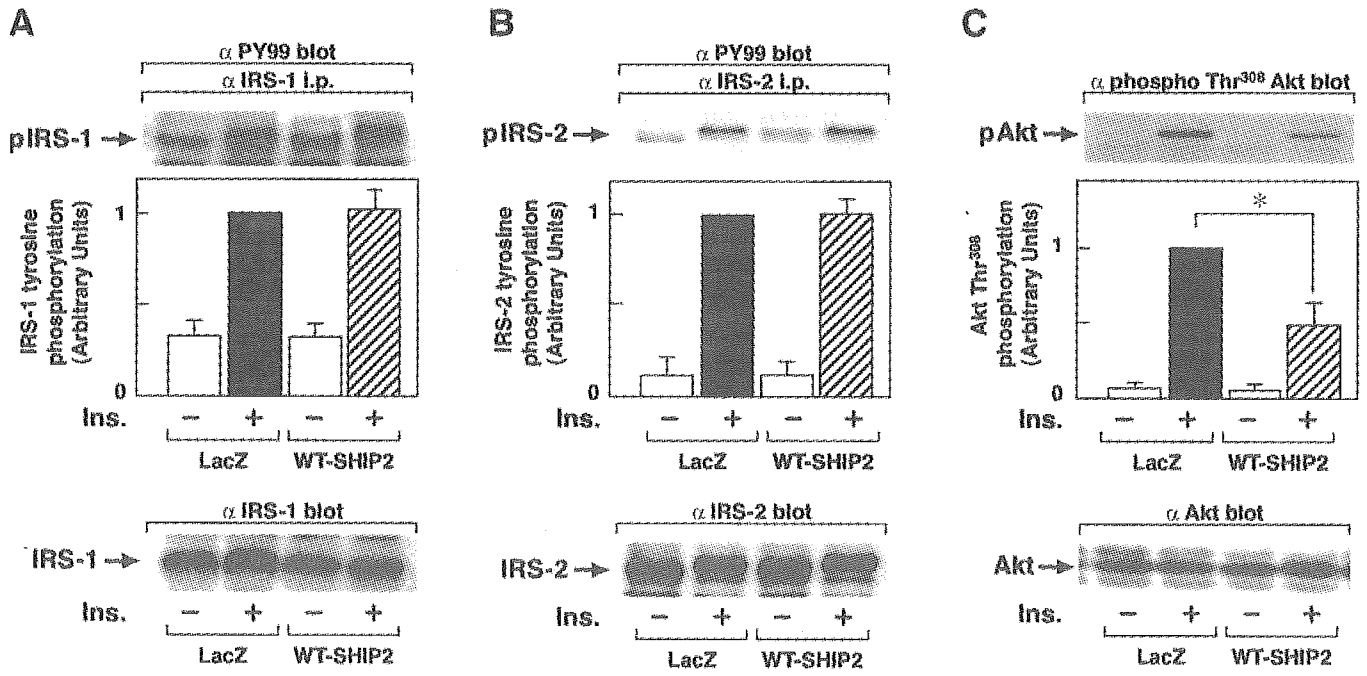

FIG. 2. Effect of WT-SHIP2 expression on insulin (Ins.)-induced phosphorylation of IRS and Akt in the liver of db/+m mice. WT-SHIP2– and LacZ-injected db/+m mice starved for 16 h were injected with insulin (5 units/kg) via the tail vein. After 5 min, the liver was excised and homogenized. Tissue samples were immunoprecipitated with anti–IRS-1 antibody (*A*) or anti–IRS-2 antibody (*B*). The precipitates were subjected to immunoblot analysis with the same antibodies or anti-phosphotyrosine antibody. The tissue samples were subjected to immunoblot analysis with anti-Akt antibody or anti–phospho-Thr^{308}–specific Akt antibody (*C*). Results are means ± SE of four separate experiments. *$P < 0.05$ vs. the amount of Akt phosphorylated in LacZ-transfected mice. i.p., intraperitoneal.

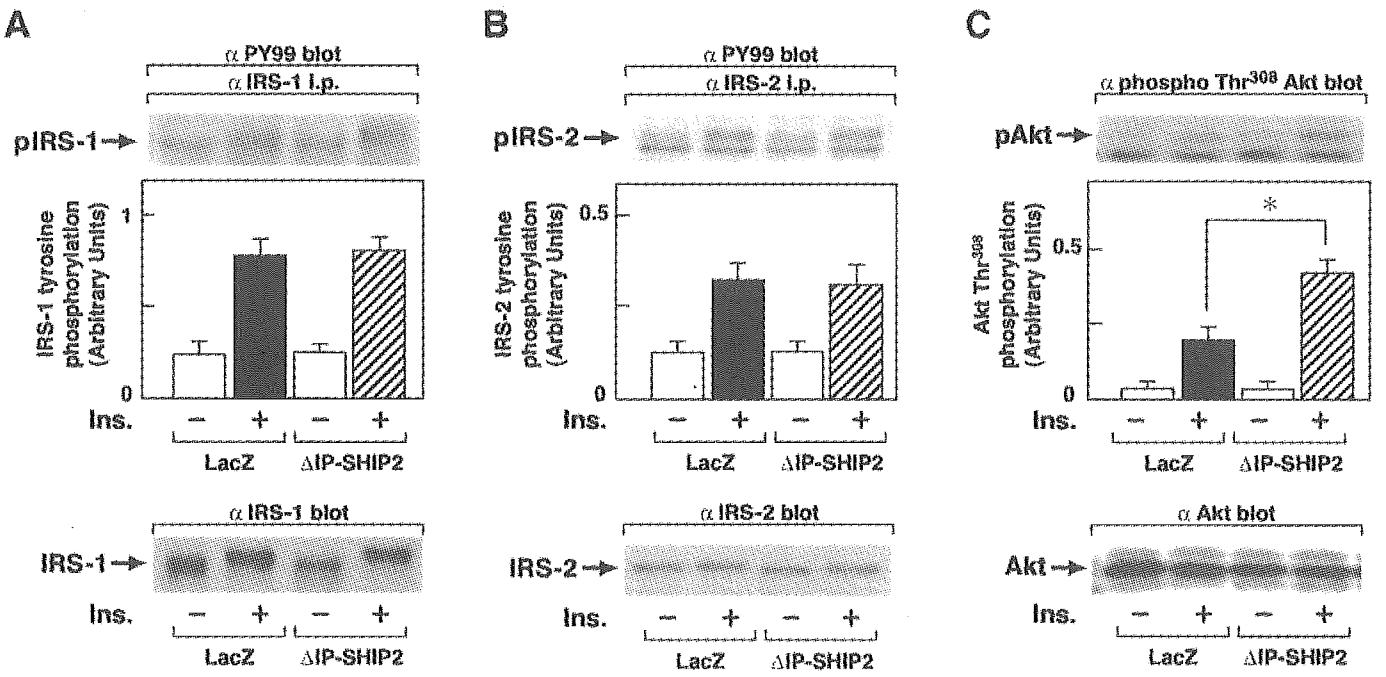

FIG. 3. Effect of ΔIP-SHIP2 expression on insulin (Ins.)-induced phosphorylation of IRS and Akt in the liver of diabetic *db/db* mice. ΔIP-SHIP2– and LacZ-injected *db/db* mice starved for 16 h were injected with insulin (5 units/kg) via the tail vein. After 5 min, the liver was excised and homogenized. Tissue samples were immunoprecipitated with anti–IRS-1 antibody (*A*) or anti–IRS-2 antibody (*B*). The precipitates were subjected to immunoblot analysis with the same antibodies or anti-phosphotyrosine antibody. The tissue samples were subjected to immunoblot analysis with anti-Akt antibody or anti–phospho-Thr^{308}–specific Akt antibody (*C*). Results are means ± SE of four separate experiments. *$P < 0.05$ vs. the amount of Akt phosphorylated in LacZ-transfected mice. i.p., intraperitoneal.

was not altered (data not shown). Consistent with the results in Fig. 2, amounts of IRS-1, IRS-2, and Akt in the liver were not changed by the expression of ΔIP-SHIP2 in *db/db* mice compared with that in LacZ-injected *db/db* mice (Fig. 3*A–C*). Insulin-induced phosphorylation of Akt at Thr^{308} was decreased in *db/db* mice to 19.7 ± 5.0% of that in control db/+m mice. Interestingly, the extent of phosphorylation was restored to 45.2 ± 4.5% by expression of ΔIP-SHIP2 in the liver of *db/db* mice (Fig. 3*C*). In addition, the degree of change in the phosphorylation of Akt well paralleled the alteration of Akt activity in both db/+m and *db/db* mice (data not shown). Furthermore, similar results were seen in 5-h–fasted mice in addition to 16-h–fasted mice (data not shown). These results indicate that SHIP2 is involved in the regulation of insulin-induced phosphorylation of Akt in the liver of both nondiabetic and diabetic mice.

Effect of SHIP2 expression on the hepatic gene expression in db/+m mice and *db/db* mice. Because the metabolic effect of insulin in the liver is mainly regulated by the hepatic expression of genes involved in gluconeogenesis, glycolysis, and fat synthesis (29), we examined the effect of liver-specific SHIP2 expression on the insulin-induced regulation of the hepatic gene expression (Fig. 4*A–D*). We performed Northern blot analysis of total RNA isolated from the liver of db/+m mice and *db/db* mice. The level of G6Pase mRNA and PEPCK mRNA in the liver was increased by 179 ± 78 and 190 ± 57%, respectively, by the liver-specific expression of WT-SHIP2 in db/+m mice. On the other hand, the abundance of GK mRNA was not altered, and that of SREBP1 mRNA was decreased by 45.0 ± 6.5% by the expression. The levels of G6Pase, PEPCK, GK, and SREBP1 mRNAs in the liver were increased by 872 ± 59, 460 ± 49, 306 ± 26, and 120 ± 16%, respectively, in LacZ-transfected *db/db* mice compared with control db/+m mice. The enhanced expression of G6Pase mRNA and PEPCK mRNA was partly reduced by 23.0 ± 8.0 and 36.0 ± 13.0%, respectively, by the liver-specific expression of ΔIP-SHIP2 in *db/db* mice compared with that of LacZ-injected *db/db* mice. Conversely, the extent of GK mRNA expression in the liver was further enhanced by 31.0 ± 9.0% in the ΔIP-SHIP2–expressing *db/db* mice. Elevated expression of SREBP1 mRNA was not changed by the expression. On the other hand, although the expression of Glut2 mRNA in the liver was increased in *db/db* mice compared with db/+m mice, neither WT-SHIP2 nor ΔIP-SHIP2 expression affected the level of Glut2 mRNA (Fig. 4*E*). In addition, the abundance of r18S RNA was equal among the samples to ensure that the same amount of total RNA was used (Fig. 4*F*).

Liver-specific expression of SHIP2 did not affect insulin-induced phosphorylation of IRS and Akt in the skeletal muscle and fat tissue of db/+m and *db/db* mice. We further investigated whether the liver-specific expression of SHIP2 affects insulin signaling in skeletal muscle and fat tissue. The level of IRS-1 or Akt did not differ in the skeletal muscle of WT-SHIP2– and LacZ-expressing db/+m mice, and that of ΔIP-SHIP2– and LacZ-expressing *db/db* mice. In addition, no apparent difference was found in the amount of basal and insulin-induced phosphorylation of IRS-1 and Akt in the skeletal muscle of WT-SHIP2– and LacZ-expressing db/+m mice and in that of ΔIP-SHIP2– and LacZ-expressing *db/db* mice (Fig. 5). Similarly, neither the amount nor the extent of insulin-induced phosphorylation of IRS-1 and Akt differed in the fat tissue of WT-SHIP2– and LacZ-expressing db/+m